

1 A competition between slicing and buckling underlies the erratic nature of paper cuts

2 Sif Fink Arnbjerg-Nielsen, Matthew D. Biviano, and Kaare H. Jensen^{*}
3 Department of Physics, Technical University of Denmark,
4 DK-2800 Kongens Lyngby, Denmark

5 (Dated: June 20, 2024)

6 By enabling the dissemination and storage of information, paper has been central to human
7 culture for more than a millennium. Its use is, however, associated with a common injury: the
8 paper cut. Surprisingly, the physics underpinning a flexible sheet of paper slicing into soft tissues
9 remains unresolved. In particular, the unpredictable occurrence of paper cuts, often restricted to
10 a limited thickness range, has not been explained. Here we visualized and quantified the motion,
11 deformation, and stresses during paper cuts, uncovering a remarkably complex relationship between
12 cutting, geometry, and material properties. A model based on the hypothesis that a competition
13 between slicing and buckling controls the probability of initiating a paper cut is developed and
14 successfully validated. This explains why paper with a specific thickness is most hazardous (65 μm ,
15 corresponding, e.g., to dot matrix paper), and suggests a probabilistic interpretation of irregular
16 occurrence of paper cuts. Stimulated by these findings, we finally show how a recyclable cutting
17 tool can harness the surprising power of paper.

19 Paper cuts are a common injury that can cause significant pain and discomfort [1]. It is endemic among literate
20 persons (globally 86% aged 15+ [2]), and may lead to severe microbial infections [3, 4]. Despite its widespread
21 occurrence, however, the physical mechanism that allows certain types of paper to cut into the skin, but precludes
22 others, remains poorly understood [5].

23 A particular mystery surrounds the link between paper thickness and the occurrence of cuts, often described as
24 unpredictable and erratic. Fine, thin, and sharp blades have long been preferred, "for bluntness is a cause of great
25 pain" (Julius Africanus, c. 200 CE [6]), and are currently in widespread use [7]. However, this principle does not hold for paper cuts. Injuries often occur while handling a magazine or office paper (thickness $t \approx 0.05 - 0.10$ mm). In contrast, tissues ($t \approx 0.03$ mm), as well as postcards ($t \approx 0.2$ mm), are generally considered safe (Fig. [1]). The restricted occurrence of paper cuts in a limited thickness range has not been explained [5].

26 In this letter, we combine experiments and theory to map the mechanics of paper cutting into a soft solid. Two parameters are explored: the paper thickness t and the slicing angle ϕ , which is a key parameter for both rigid blades [8, 10], wire cutters [11, 12] and paper cuts [13]. Our experiments reveal that for paper blades, a competition between slicing and buckling controls the cutting process. This provides a simple framework for understanding the erratic nature of paper cuts, and lays the foundation for physics-informed design of paper-based blades.

49 Methods

50 To quantify if and when paper can cut a soft solid, we attempted to slice into a piece of freshly prepared gelatin using a variety of paper sheets (Fig. [1]). The paper speci-

51 mens were chosen for broad coverage and availability (see Supplemental Information, Table S1 [14]). The standardized paper sample was a rectangle of length $\ell = 10$ cm and thickness $t = 0.025 - 0.25$ mm sandwiched between two 3D-printed elements parallel to the paper edge (Fig. [2A]). When handling paper, for instance, when turning the page of a journal, a book, or a newspaper, we often fix the sheet using one finger while trying to peel or lift the edge using another finger. The characteristic paper height (h) can thus be objectively defined as the typical thickness of a finger. The value used here ($h = 14$ mm) corresponds to the size of an index finger of Western children and adults [15]. The elastic modulus $E_s \approx 3$ kPa of the gelatin (Bloom 230, 10% wt, dissolved in water at 75–100°C and set for 26–29 h at 20°) was measured using a rectangular punch indentation test [16] (Appendix B, Fig. [6]). The gelatin sample was a slab of length $L = 7$ mm, thickness $T = 40$ mm, and height $H = 10$ mm, fixed at the bottom and on the two sides parallel to the paper blade. The sample dimensions and properties were again chosen based on human limb sizes [17, 18]. The cutting edge remained parallel to the cutting surface along the y -axis throughout the experiments (Fig. [2A]). The cutting speed (typically 2.8 mm/s) was controlled by mounting the paper clamp on a 2-axis stage driven by servomotors (MPC-200/MP-285, Sutter Instruments, USA). We varied the cutting angle ϕ by modifying the y - and z -velocity components to explore the role of shear in the cutting process from $\phi = 5$ degrees (motion almost parallel to the surface) to $\phi = 90$ degrees (normal motion). The vertical indentation depth $d = 2$ mm of the paper sheet post contact with the gelatin block was kept constant. The deformation and cutting processes were recorded with a video camera (camera: acA1920-uc, Basler AG, Germany, lens: AF-P DX Nikkor 18-55mm f/3.5-5.6G VR, Nikon, Japan). Normal (σ_n) and shear (σ_t) stresses induced by the slic-

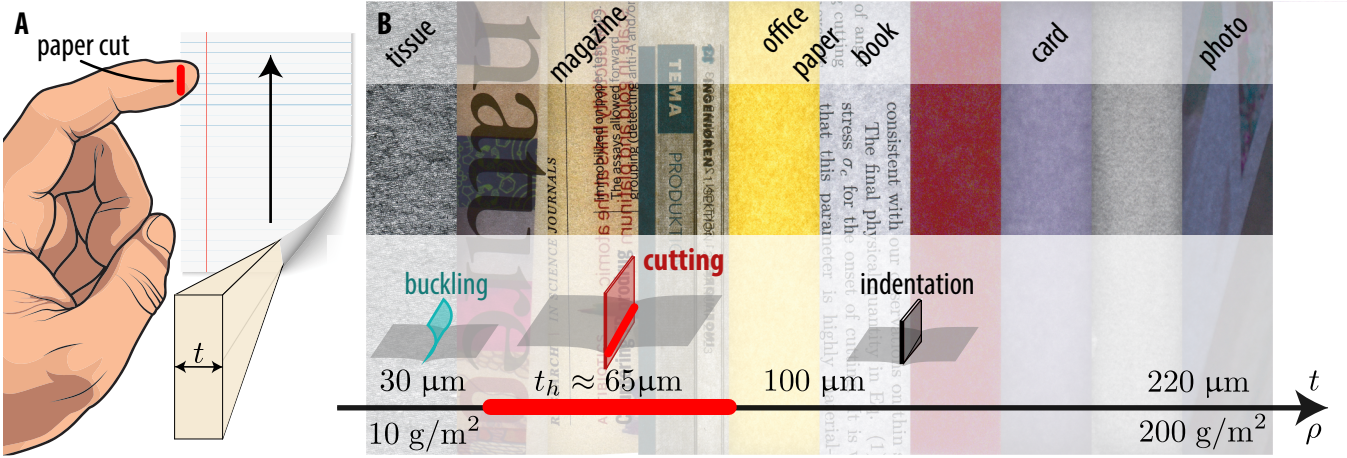


FIG. 1. The physics of paper cuts. (A) Paper cuts are a common injury that can occur if skin contacts a sheet of paper (thickness t , area density ρ). It causes significant pain and discomfort and is often associated with a slicing motion (arrow). The underlying physical processes remain poorly understood. (B) However, it is well-established that cuts frequently occur in the thickness range $t = 0.05 - 0.1$ mm (this range includes magazines and office paper) [5], while the thinner and thicker paper is relatively safe. We propose that a competition between slicing and buckling determines which paper types can cut. If the sheet is too thin, it buckles and loses structural integrity before initiating a fracture. In contrast, thicker sheets smoothly indent the surface and distribute the load over a greater area. The slicing motion enhances the likelihood of cutting, which peaks at the most hazardous thickness $t_h \approx 65 \mu\text{m}$ (see Fig. 2).

ing motion ($\tan \phi = \sigma_n / \sigma_t$) were measured using two₁₉ orthogonally mounted force sensors (TAL221 100g load₂₀ cell, SparkFun Electronics, USA, amplifier: Mini Weight₂₁ Unit HX711, M5Stack, China). The Young's modulus₂₂ of paper was measured by a cantilever bending test [19].₂₃ See the Supplemental Information (Data S1) for CAD₂₄ drawings [14].

tangential load increases super-linearly after the cut is initiated. The sheet remains rigid during the experiment but cleanly cuts into the sample, leaving a permanent scar on the gelatin surface. Because the comparatively thinner sheet applied nearly the same peak force to the slab, the peak applied stress σ_a (force per contact area), exceeded the critical level $\sigma_{n,c}$ required to initiate cutting in this case.

Results

Experiments Each paper sample's cutting dynamics₁₂₉ are unique, but clear patterns allow us to divide the data₁₃₀ into three rough categories (Fig. 2, Appendix A, Fig. 5)₁₃₁ and Supplemental video S1 [14]). To unpack the relevant₁₃₂ physical processes, we begin by considering the performance₁₃₃ of a relatively thick sheet ($t = 0.22$ mm) at a₁₃₄ fixed slicing angle, say $\phi \approx 15$ degrees (Fig. 2D). In this₁₃₅ case, the normal stress σ_n increases rapidly as the paper₁₃₆ pushes against the gelatin until reaching peak applied₁₃₇ stress, σ_a , while the tangential load σ_t grows but remains₁₃₈ comparatively small. Although the gelatin is strongly de-₁₃₉ formed in the vertical direction (Supplemental video S1₁₄₀ [14]), the paper retains its shape, and a visual inspection₁₄₁ of the substrate surface before and after the experiment₁₄₂ reveals that no cutting has occurred (Appendix A, Fig.₁₄₃ 5). Apparently, the applied stress σ_a remained below the₁₄₄ critical value $\sigma_{n,c}$ required to initiate cutting (see, e.g.,₁₄₅ [8, 11, 20]).

The final data category captures the behavior of relatively thin sheets (e.g., $t = 0.03$ mm, $\phi = 15$ degrees). Here, the tangential force again increases linearly, while the normal load trajectory has a distinct kink (Fig. 2B): Shortly following contact, the thin sheet is bent out of shape by the applied load. It then slides along the slab, sometimes leaving minor residual abrasion damage on the surface. Presumably, the unsuccessful cutting results from the paper buckling at the stress σ_b below the critical cutting value $\sigma_{n,c}$.

Having established the three basic data categories (indentation, cutting, and buckling), we will now examine the influence of the slicing angle ϕ . To facilitate this discussion, we position our data in a phase diagram as a function of the sheet thickness t and the cutting angle ϕ (Fig. 3). The aforementioned transition from indentation to cutting and buckling with diminishing paper thickness is consistently observed for angles in the range $\phi = 10 - 25$ degrees. We did not detect cutting for angles $\phi > 25$ degrees. Also, the data suggest that the range of paper thicknesses able to cut broadens dramatically when the slicing angle diminishes. However, the physical reason for the data tripartition remains unknown.

97

127

128

129

130

131

132

133

134

135

136

137

138

139

140

141

142

143

144

145

146

147

148

149

150

151

152

153

154

155

156

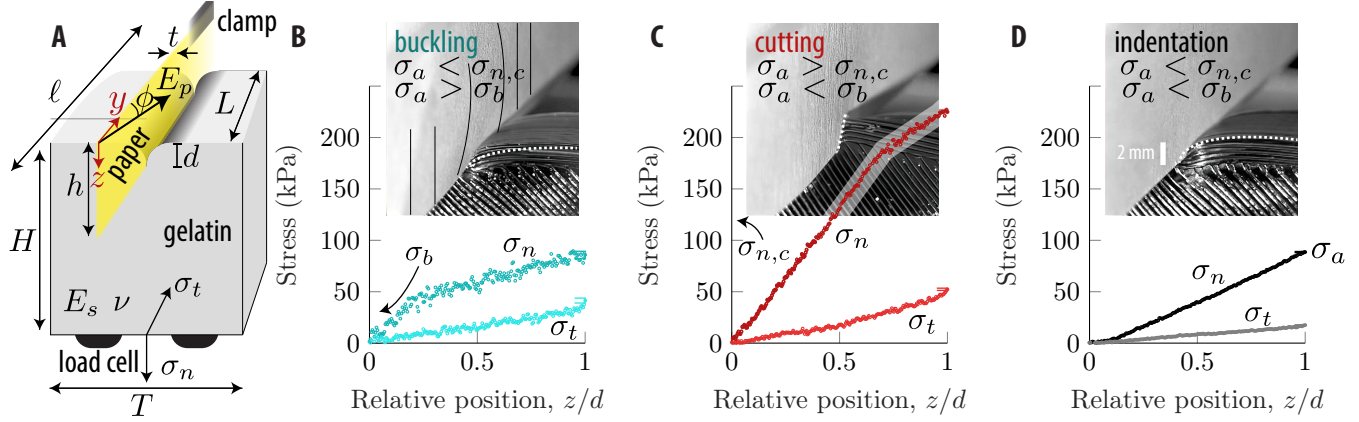


FIG. 2. Experimental setup and data classification scheme. (A) Schematic of the experiment used to quantify contact processes between a soft solid and a sheet of paper in relative motion. The standardized paper and gelatin samples were held by 3D-printed clamps. The vertical indentation depth, d , the speed (arrow), and the slicing angle ϕ of the paper sheet were controlled using a micromanipulator. A video of each experiment was recorded and the stresses (normal (σ_n) and tangential (σ_t) to the gelatin surface) were measured using two load cells. (B-D) Representative data illustrating three regimes. (B) Thin paper ($t = 30 \mu\text{m}$, $\phi = 15$ degrees) buckles because the normal load exceeds the buckling threshold σ_b before reaching peak applied stress, $\sigma_a > \sigma_b$. (C) Intermediate paper ($t = 65 \mu\text{m}$, $\phi = 15$ degrees) cuts because the cutting threshold $\sigma_{n,c}$ is exceeded before reaching σ_b or σ_a . (D) Finally, thick paper ($t = 220 \mu\text{m}$, $\phi = 15$ degrees) indents the surface because the dispersed normal force is insufficient to breach the surface or buckle the paper. (See also supplemental Video S1 [14] and additional details in the text)

Physical model To rationalize the experimental data,¹⁷⁹ we develop a simple mathematical model of paper cutting¹⁸⁰ into a soft material. The process can be studied in full¹⁸¹ detail using direct numerical simulations, e.g., with finite¹⁸² element methods [8, 11, 12]. However, here we focus¹⁸³ on the fundamental physical phenomena and attempt to derive scaling relations to explain the phase diagram's¹⁸⁴ critical features (Fig. 3).

We begin by stating the basic fact that for successful¹⁸⁵ cutting, the normal stress σ_n must, at some point during¹⁸⁶ the cutting attempt, exceed the critical threshold $\sigma_{n,c}$ ¹⁸⁷ required to cut. On the other hand, it should not grow¹⁸⁸ larger than the buckling limit σ_b at which the paper loses¹⁸⁹ most ability to convert the vertical strain into stress. Re-¹⁹⁰call that during the slicing process, σ_n increases from zero¹⁹¹ (initial contact) to its peak value σ_a when the paper has¹⁹² moved a distance d along the vertical axis (Fig. 2D). The¹⁹³ peak applied stress must therefore obey the inequality¹⁹⁴

$$\sigma_{n,c} < \sigma_a < \sigma_b, \quad (1)$$

which, as shown below, explains the three distinct regions¹⁹⁷ in the phase diagram (Fig. 3).

To unpack the physical meaning of the cutting inequality¹⁹⁸ (Eq. (1)), we begin by considering the magnitude of¹⁹⁹ the peak applied stress, σ_a . The interaction between the²⁰⁰ paper sheet and the gelatin sample can be approximated²⁰¹ as a uniform indentation of a rigid rectangular punch into²⁰² an elastic half-space [16], in which case the average peak²⁰³ applied stress is

$$\sigma_a = \frac{\pi}{2 \ln 2} \frac{E_s}{1 - \nu^2} \frac{d}{t}, \quad (2)$$

where $\nu \approx 0.5$ is Poisson's ratio (Fig. 2A). As expected, the peak applied stress $\sigma_a \sim t^{-1}$ scales inversely with the paper thickness t and linearly with the indentation depth d (c.f., Hooke's law). Similarly, the buckling threshold stress σ_b can be found from beam theory [21]

$$\sigma_b = \kappa E_p \frac{t^2}{h^2}, \quad (3)$$

where $E_p \approx 7.5$ GPa is the elastic modulus of paper in the thin range of the tested range (Table S1), t is the thickness, and h is the height of the paper blade (Fig. 1A). The prefactor $\kappa = \pi^2/(12K^2)$ is determined by the boundary conditions for the buckling blade. In our case, one end is pinned while the other is fixed, corresponding to $K \approx 0.70$ such that $\kappa \approx 1.68$. The scaling $\sigma_b \sim t^2$ is consistent with our observations on thin sheets (Appendix C, Fig. 7). It is possible to consider plate-like flexural instabilities using detailed numerical simulations (e.g., [22]), but we will not do that here.

The final physical quantity in the inequality (1) is the normal stress $\sigma_{n,c}$ at the onset of cutting. Soft solids can typically resist large compressive stresses but fail under a critical tensile stress $\sigma_{t,c}$ that might result from a combination of compression and/or shear. For gelatin and human skin, cutting stresses are of the order 0.1–1 MPa [23, 24]. It is well-established that the tensile stress required to initiate cutting depends on the fracture toughness and Young's modulus, and that it can be affected by, e.g., aging and environmental factors such as temperature and humidity [11, 12, 23, 25–27]. Surface abrasion caused by dynamic (sliding) friction may also lower the

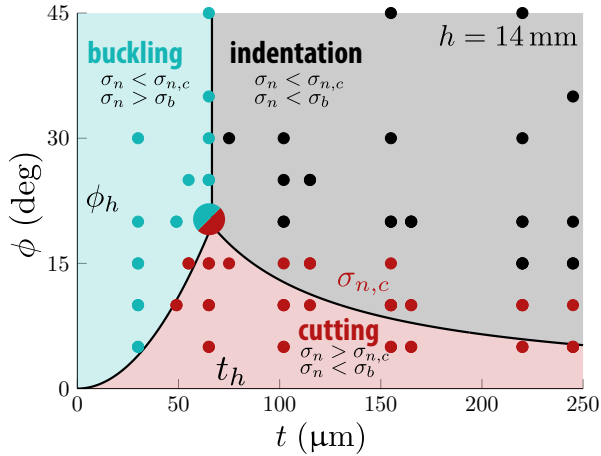


FIG. 3. A competition between slicing and buckling govern paper cuts. The phase diagram shows the outcome of each experiment (dots) as a function of thickness t and slicing angle ϕ . The outcome of a cutting attempt depends on how the thresholds relate to each other. If $\phi < \phi_h$, there exists a range of thicknesses for which $\sigma_{n,c}$ is lower than both σ_a and σ_b where cutting is observed. When the slicing angle ϕ is sufficiently small, nearly all types of paper cuts (red shaded domain, label: cutting). However, the probability peaks at the most hazardous thickness $t_h \approx 65 \mu\text{m}$ (between printed magazines and office paper) and angle $\phi_h \approx 20$ degrees. Outside this zone, the peak applied stress either exceeds the buckling limit (label: buckling) or simply causes an indentation (label: indentation) (top-right). The mechanical model (Eq. 14) is consistent with observations (solid lines mark model transitions between domains). Error bars: $t \pm 5 \mu\text{m}$ and $\phi \pm 2$ degrees. See additional details in the text.

combinations of paper thickness and slicing angle can generate enough stress to cut into the substrate. Specifically, for a fixed slicing angle ϕ , the cutting threshold normal stress $\sigma_{n,c}(\phi)$ is a constant (Eq. 4). However, the peak applied stress $\sigma_a \sim t^{-1}$, increases when the paper thickness t diminishes, while the paper becomes more prone to buckling. The outcome thus depends on which of the two thresholds will be reached first: cutting $\sigma_{n,c}$ (Eq. 4) or buckling $\sigma_b \propto t^2$ (Eq. 3). The most hazardous paper thickness t_h (for which cutting is possible for the greatest range of angles) corresponds to the case where the peak applied stress, buckling threshold, and cutting threshold are equal, i.e., $\sigma_a = \sigma_b = \sigma_{n,c}$. Equating Eq. 23 leads to an expression for the most hazardous paper thickness in terms of the system parameters

$$t_h = \alpha \left(\frac{1}{1-\nu^2} \frac{E_s}{E_p} h^2 d \right)^{1/3} \approx 65 \mu\text{m} \quad (5)$$

where $\alpha = [\pi/(2\kappa \ln 2)]^{1/3} \approx 1.1$ is a numerical constant.

The largest angle at which cutting is observed for a given thickness t , i.e. the line delimiting the cutting regime from the other domains in the phase diagram (Fig. 3) is given by:

$$\phi_c(t) = \begin{cases} \kappa \frac{E_p}{\sigma_{t,c}} \frac{t^2}{h^2} & \text{if } t \leq t_h \\ \frac{\pi}{2 \ln 2(1-\nu^2)} \frac{E_s}{\sigma_{t,c}} \frac{d}{t} & \text{if } t \geq t_h \end{cases} \quad (6)$$

From this follows $\phi_h = \phi_c(t_h) \approx 19$ degrees, i.e. no paper will cut at angles larger than 19 degrees.

Notably, the most hazardous thickness t_h scales relatively weakly (i.e., to the 1/3-power) with the material and geometric parameters. In most realistic cases, it therefore deviates relatively little from the estimate $t_h \approx 65 \mu\text{m}$, near, for instance, magazines and dot matrix paper (Supplemental Information, Table S1 14). It should be noted that the free height h influences the transitions between domains in the phase diagram. A phase diagram for $h = 28 \text{ mm}$ is not inconsistent with the prediction that t_h increases and ϕ_h decreases with h (Appendix E, Fig. 9). However, validation of the scaling laws $t_h \sim h^{2/3}$ and $\phi_h \sim h^{-2/3}$ require additional experiments.

We end this section by providing a broader perspective on the paper cutting process and a statistical interpretation of the phase diagram (Fig. 3): paper cuts are associated with a range of activities across home, school, office, and industry environments. Although certain angles (ϕ) between finger and paper may be connected to particular activities, it is difficult to argue for the strong prevalence of any specific angle(s). Inspired by statistical mechanics, we consider the slicing angle ϕ as a random variable with a uniform probability distribution and examine the cutting probability $p(t)$ at a fixed paper thickness t across a range of angles $0 < \phi < \pi/2$. The likelihood of cutting during handling of the paper can then be described as the

208 cutting stress. However, the residual abrasion damage 209 did not exceed the imperfections caused by the fabrica- 210 tion process. Evidence thus does not suggest that friction 211 in the parallel motion played a critical role in the onset 212 of cutting. 213

For combined normal and tangential loading, the 214 largest tensile stress equals the shear stress σ_t 11. An 215 essential feature of slicing soft materials is therefore that 216 the normal stress $\sigma_{n,c}$ necessary for cutting (c.f., Eq. (1)) 217 varies with the slicing angle ϕ because of the direct cou- 218 pling to the shear component (recall $\sigma_n = \sigma_t \tan \phi$). We 219 can therefore approximate the critical normal stress by a 220 linear angular dependence 221

$$\sigma_{n,c} \approx \sigma_{t,c} \phi. \quad (4)$$

222 Experimentally, the linear relation is consistent with ex- 223 perimental data beyond the validity of the small angle 224 approximation ($\sigma_{t,c} = 0.84 \text{ MPa}$, Appendix D, Fig. 8). 225 At $\phi \approx 30$ degrees, the Taylor expansion deviates with 226 10%. We note that cutting phenomena at $\phi = 0$ degrees 227 are not described by this model. 228

When taken together, Eqs. (14) reveal a basic physical 229 explanation of the phase diagram domains: only certain 230

280 probability of paper handling at an angle below $\phi_c(t)$:

$$281 \quad p(t) = \frac{\phi_c(t)}{\pi/2}, \quad (7)$$

282 Eq. (7) provides a potential explanation for the erratic
 283 nature of paper cuts. As seen in Fig. 3 cutting mostly
 284 occurs for angles $\phi \leq 15$ degrees. However, at or near the
 285 most hazardous paper thickness t_h (Eq. (5)), there is a
 286 much greater chance of injury, $p(t_h) = \frac{\phi_c(t_h)}{\pi/2}$. Expressed
 287 in all system parameters, the change of injury at the most
 288 hazardous thickness is

$$289 \quad p(t_h) = \frac{1}{\pi/2} \frac{\kappa\alpha^2}{(1-\nu^2)^{2/3}} \frac{(E_p^{1/2} E_s)^{2/3}}{\sigma_{t,c}} \left(\frac{d}{h}\right)^{2/3} \approx 21\% \quad (8)$$

290 When handling the most hazardous paper, the chance
 291 of injury is thus roughly one in five averaged over many
 292 random interactions.

293 Discussion and conclusion

294 A fairly comprehensive picture of the physical pro-
 295 cesses that may reduce (or enhance) the dangers of paper
 296 cuts has emerged. First and foremost, we provide a ra-³²⁷
 297 tionale for the surprising observation that slicing only³²⁸
 298 occurs when the paper edge is fine, but not too thin.³²⁹
 299 The reason is that cutting into soft tissues requires a cer-³³⁰
 300 tain critical force. However, if the paper is overly fine, it³³¹
 301 buckles under the load before cutting can occur.³³²

302 These results allow us to assess the relative safety of³³³
 303 various product categories broadly. While tissues, books,³³⁴
 304 and photos are generally safe, we cannot rule out certain³³⁵
 305 risks of using office paper or magazine. In the future, pa-³³⁶
 306 per manufacturers, printers, and publishing companies
 307 may wish to consider this during the product design pro-³³⁷
 308 cess.

309 It is worth pointing out, however, that the habits and³³⁸
 310 dexterity of the user also play a role. In particular, most³³⁹
 311 paper cuts can be avoided by adhering to a strict near-³³⁹
 312 normal-contact regimen (i.e., $\phi > \phi_h \approx 20$ degrees),³⁴⁰
 313 which minimizes the cutting likelihood. Regardless, we³⁴¹
 314 stress that more work is needed to assess the influence³⁴²
 315 of the azimuthal slicing angle, and the relative safety of³⁴³
 316 composite paper products, such as corrugated cardboard.³⁴⁵

317 Identifying the most hazardous paper thickness may³⁴⁶
 318 also allow for novel applications in cases where cutting is³⁴⁷
 319 desirable. Indeed, we speculate that paper blades may of-³⁴⁸
 320 fer a substitute for conventional metallic knives in cases³⁴⁹
 321 such as cooking and dining [28], and, perhaps, in the³⁵⁰
 322 textile industry and home gardening. The regular occur-³⁵¹
 323 rence of paper cuts also demonstrates that paper may³⁵²
 324 have a future role in transdermal drug delivery [29] if,³⁵³
 325 for instance, the drug is mixed into the paper matrix.³⁵⁵
 326 Stimulated by these ideas, we designed and 3D printer³⁵⁶

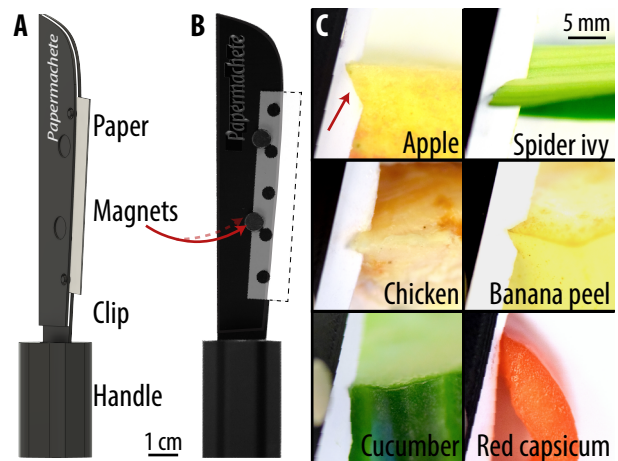


FIG. 4. The Papermachete uses discarded traction sections of dot-matrix paper as a blade. (A) Technical drawing and (B) photograph of the recyclable paper-knife. The single-use paper blade is fixed in the clip by magnets while the handle facilitates convenient use. (C) The Papermachete can cut into a variety of plant and animal-based products. The cuts were performed by hand at the slicing angle of $\phi \approx 10$ degrees at speeds of approximately 1 cm/s in the direction of the arrow.

the *Papermachete* (Fig. 4A,B), which utilizes discarded traction sections of dot-matrix paper as a blade. (See the Supplemental Information for design files [4]). The Papermachete easily cuts into most soft plant and animal-based products (Fig. 4C); it is, however, not suitable for, e.g., wood carving and spreading butter. Despite its seemingly mundane nature, studying the physics of paper cuts has revealed a surprising potential use for paper in the digital age: not as a means of information dissemination and storage, but rather as a tool of destruction.

* khjensen@dtu.dk

- [1] L. Peterson, L. Saldana, and N. Heiblum, Quantifying tissue damage from childhood injury: The minor injury severity scale, *Journal of Pediatric Psychology* **21**, 251 (1996).
- [2] M. Roser and E. Ortiz-Ospina, Literacy, Our World in Data (2016), <https://ourworldindata.org/literacy>.
- [3] S. L. DeBoer and D. Zeglin, Necrotizing fasciitis: Even with optimal treatment, the mortality rate is 40%, *AJN The American Journal of Nursing* **101**, 37 (2001).
- [4] A. H. Milby, N. D. Pappas, J. O'Donnell, and D. J. Bozentka, Sporotrichosis of the upper extremity, *Orthopedics* **33**, 273 (2010).
- [5] S. Mirsky, The unkindest cut, *Scientific American* **306**, 80 (2012).
- [6] J. C. McKeown, *A Cabinet of Ancient Medical Curiosities: Strange Tales and Surprising Facts from the Healing Arts of Greece and Rome* (Oxford University Press, 2016).
- [7] D. Zhou and G. McMurray, Modeling of blade sharpness

- and compression cut of biomaterials, *Robotica* **28**, 311–421 (2010). 421
 [8] S. Mora and Y. Pomeau, Cutting and slicing weak solids, 422
Physical Review Letters **125**, 038002 (2020). 424
 [9] A. G. Atkins, X. Xu, and G. Jeronimidis, Cutting, by 425
 ‘pressing and slicing,’ of thin floppy slices of materials il-426
 lustrated by experiments on cheddar cheese and salami, 427
Journal of Materials Science **39**, 2761 (2004). 428
 [10] A. Spagnoli, R. Brighenti, M. Terzano, and F. Artoni, 429
 Cutting resistance of soft materials: Effects of blade in-430
 clination and friction, *Theoretical and Applied Fracture* 431
Mechanics **101**, 200 (2019). 432
 [11] E. Reyssat, T. Tallinen, M. Le Merrer, and L. Mahadevan, 433
 Slicing softly with shear, *Physical review letters* **109**, 434
 244301 (2012). 435
 [12] Y. Liu, C.-Y. Hui, and W. Hong, A clean cut, *Extreme* 436
Mechanics Letters **46**, 101343 (2021). 437
 [13] A. Atkins, Slice-push, formation of grooves and the scale 438
 effect in cutting, *Interface Focus* **6**, 20160019 (2016). 439
 [14] See Supplemental Material at [URL will be inserted by 440
 publisher] for design files of experimental setup and *Pa-441
 permachete* and video of cutting experiments. 442
 [15] P. W. Johnson and J. M. Blackstone, Children and 443
 gender-differences in exposure and how anthropometric 444
 differences can be incorporated into the design of com-445
 puter input devices, *Scandinavian Journal of Work, En-446
 vironment & Health* , 26 (2007). 447
 [16] P. Brothers, G. Sinclair, and C. Segedin, Uniform in-448
 dentation of the elastic half-space by a rigid rectangular 449
 punch, *International Journal of Solids and Structures* **13**, 450
 1059 (1977). 451
 [17] M. Oldfield, D. Dini, T. Jaiswal, and F. Rodriguez y 452
 Baena, The significance of rate dependency in blade in-453
 insertions into a gelatin soft tissue phantom, *Tribology In-454
 ternational* **63**, 226 (2013), the International Conference 455
 on BioTribology 2011. 456
 [18] S. Komandur, P. W. Johnson, R. L. Storch, and M. G. 457
 Yost, Relation between index finger width and hand 458
 width anthropometric measures, in *2009 Annual Interna-459
 tional Conference of the IEEE Engineering in Medicine 460
 and Biology Society* (IEEE, 2009) pp. 823–826. 461
 [19] B. Lautrup, *Physics of continuous matter: exotic and ev-462
 eryday phenomena in the macroscopic world* (CRC press, 463
 2011). 464
 [20] S. Fakhouri, S. B. Hutchens, and A. J. Crosby, Puncture 465
 mechanics of soft solids, *Soft Matter* **11**, 4723 (2015). 466
 [21] S. P. Timoshenko and J. M. Gere, *Theory of elastic sta-467
 bility* (Courier Corporation, 2009). 468
 [22] T. Barois, I. Jalisse, L. Tadrist, and E. Virot, Transi-469
 tion to stress focusing for locally curved sheets, *Physical 470
 Review E* **104**, 014801 (2021). 471
 [23] M. Czerner, L. A. Fasce, J. F. Martucci, R. Ruseckaite, 472
 and P. M. Frontini, Deformation and fracture behavior 473
 of physical gelatin gel systems, *Food Hydrocolloids* **60**, 474
 299 (2016). 475
 [24] O. A. Shergold and N. A. Fleck, Experimental investiga-476
 tion into the deep penetration of soft solids by sharp and 477
 blunt punches, with application to the piercing of skin, 478
Journal of Biomedical Engineering **127**, 838 (2005). 479
 [25] M. Terzano, A. Spagnoli, and P. Stähle, A fracture me-480
 chanics model to study indentation cutting, *Fatigue &* 481
Fracture of Engineering Materials & Structures **41**, 821 482
 (2018). 483
 [26] A. Spagnoli, M. Terzano, R. Brighenti, F. Artoni, and 484
 P. Stähle, The fracture mechanics in cutting: A compa-485
 rative study on hard and soft polymeric materials, *Inter-486
 national Journal of Mechanical Sciences* **148**, 554 (2018). 487
 [27] V. Normand, S. Muller, J.-C. Ravey, and A. Parker, Gelati-488
 tion kinetics of gelatin: A master curve and network mod-489
 eling, *Macromolecules* **33**, 1063 (2000). 490
 [28] H. N. Patil and P. Sinhal, A study on edible cutlery: An 491
 alternative for conventional ones, *Atithya: A Journal of 492
 Hospitality* **4**, 45 (2018). 493
 [29] M. R. Prausnitz and R. Langer, Transdermal drug deliv-494
 ery, *Nature biotechnology* **26**, 1261 (2008). 495
 [30] R. Taylor John, *An introduction to error analysis* (Uni-496
 versity Science Books, 1997). 497
 [31] N. Taberlet, J. Ferrand, É. Camus, L. Lachaud, and 498
 N. Plihon, How tall can gelatin towers be? an introduc-499
 tion to elasticity and buckling, *American Journal of 500
 Physics* **85**, 908 (2017). 501
 [32] A. Forte, F. D’amicco, M. Charalambides, D. Dini, and 502
 J. Williams, Modelling and experimental characterisation 503
 of the rate dependent fracture properties of gelatine gels, 504
Food Hydrocolloids **46**, 180 (2015). 505
 [33] A. D. Doyle and J. Lee, Simultaneous, real-time imaging 506
 of intracellular calcium and cellular traction force pro-507
 duction, *Biotechniques* **33**, 358 (2002). 508
 [34] A. Bot, I. A. van Amerongen, R. D. Groot, N. L. Hoek-509
 stra, and W. G. Agterof, Large deformation rheology of 510
 gelatin gels, *Polymer Gels and Networks* **4**, 189 (1996). 511

448

Appendix A: Surface characterization

449 Experiments are performed to elucidate the link between paper thickness and the occurrence of paper cuts.
 450 An attempt to slice into a gelatin block with a sheet of paper is made. The interaction is recorded and tangential
 451 and normal stresses are measured. Each attempt is categorized. First, we introduce the three rough categories:
 452 buckling of the paper, cutting and indentation into the soft gelatin. Both video (Supplemental Information [4])
 453 and visual inspection of the substrate surface (Fig. 5) after the experiment are used to determine the cutting
 454 dynamics. While the contact between paper sheet and gelatin might leave residual abrasions even though buckling
 455 or indentation is observed, they are distinguishable from the slashed surface appearing after a cut.
 456

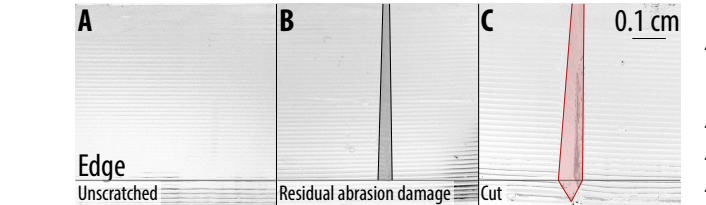


FIG. 5. Definitions of surface characteristics after experiment. The horizontal line is the edge and is included to demonstrate the cut into the sample.

463 Appendix B: Young's modulus of gelatin

464 The outcome of the interaction between a sheet of paper and a substrate depends in part on the softness of
 465 the substrate. Young's modulus of the gelatin, E_s , is
 466 measured using a normal-indentation-test using a rectangular indenter attached to a vertical stage. The in-
 467 dentor (a sheet of paper) traveled $d \approx 2$ mm into the
 468 gelatin slab. Experiments are performed with indenters
 469 of thickness $t = 0.076\text{--}0.245$ mm and no buckling was ob-
 470 served. E_s is determined by fitting data to a contact me-
 471 chanics model describing the relation between stress and
 472 strain (indentation depth) for a rigid rectangular punch
 473 in contact with an elastic half-space (Eq. 2) [16]. An
 474 unweighted least-squares linear fit with no intercept be-
 475 tween measured applied stress, σ_a , and the normalized
 476 strain, $\pi d/(2 \ln 2(1 - \nu^2)t)$ is performed [30] (Fig. 6). The
 477 fitted slope is $E_s = 3.13 \pm 0.08$ kPa. Data compares
 478 reasonably well with the linear model (Fig. 6).
 479

480 This modulus is relatively small compared to values
 481 obtained by, e.g., Taberlet *et al.* and Forte *et al.*, who
 482 observed $E_s \approx 10\text{--}80$ kPa. However, it has been demon-
 483 strated that the elastic modulus is affected by tempera-
 484 ture [33] and aging [34] (see also [31]). We therefore spec-
 485 ulate that the difference is due to the specific production
 486 and setting conditions used in the present study.
 487

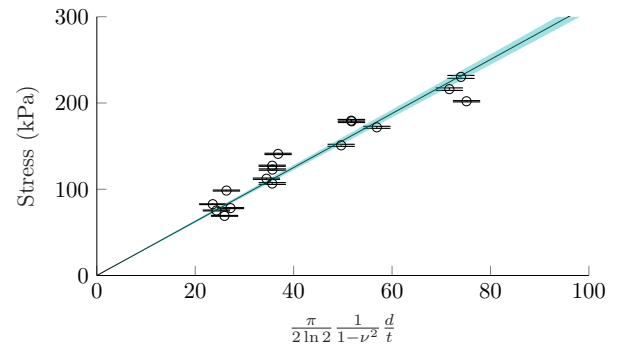


FIG. 6. Measured maximum applied stress σ_a plotted as a function of relative indentation depth d/t (dots). An unweighted least-squares to Eq. 2 yields the estimate $E_s = 3.13 \pm 0.08$ kPa (solid line).

488 Appendix C: Validity of Euler's buckling equation

Complex dynamics arise when the sheet buckles against the gelatin. To rationalize the experimental data, we employ the simple Euler's beam theory (Eq. 3). To determine the validity of this result, we measure the buckling force and compare it to the model, which stipulates $F_b \sim E_p t^3 w/h^2$. Here, E_p is the paper's elastic modulus, t and w its thickness and width, and h the free height of the sheet (Fig. 1). Data (Fig. 7) compare reasonably well with the simple model. Based on this result, we propose that effects such as complex forces due to a limited contact line and flexural instabilities can be neglected.

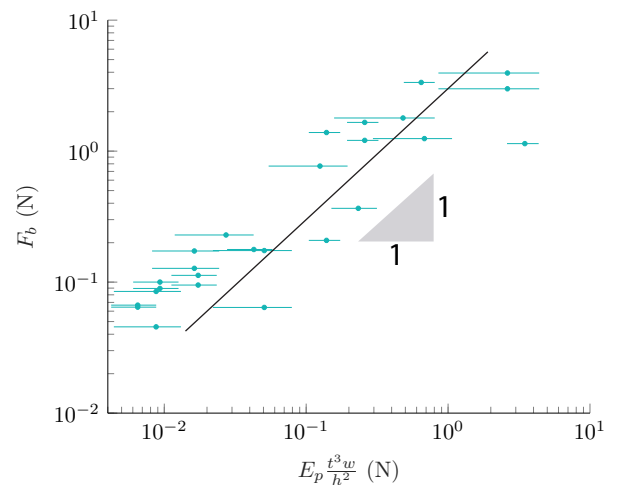


FIG. 7. Experimentally measured buckling force compared to Euler's beam equation, which stipulates $F_b \sim E_p t^3 w/h^2$. Here, E_p is the paper's elastic modulus, t and w its thickness and width, and h the free height of the sheet (Fig. 1 in the paper). Data compare reasonably well with the simple model.

Appendix D: Critical cutting stress

The critical cutting stress threshold must be exceeded for cutting to occur. At cutting onset, the critical stresses are respectively denoted $\sigma_{n,c}$ and $\sigma_{t,c}$, where $\sigma_{n,c} = \sigma_{t,c} \tan \phi$. For small angles, this is approximately $\sigma_{n,c} \approx \sigma_{t,c} \phi$. To investigate whether the small angle approximation is valid, we measure $\sigma_{n,c}$ for angles in the range $\phi = 30 - 90$ degrees. These results are plotted alongside data obtained by Reyssat *et al.* (Fig. 8). While the small angle approximation is not inconsistent with experimental data beyond its classical validity, our cutting attempt only yields cutting up to $\phi = 20$ degrees, where the deviation from the full expression is $\approx 4\%$. For the experimentally relevant angles, the linear model should sufficiently predict the cutting thresholds.

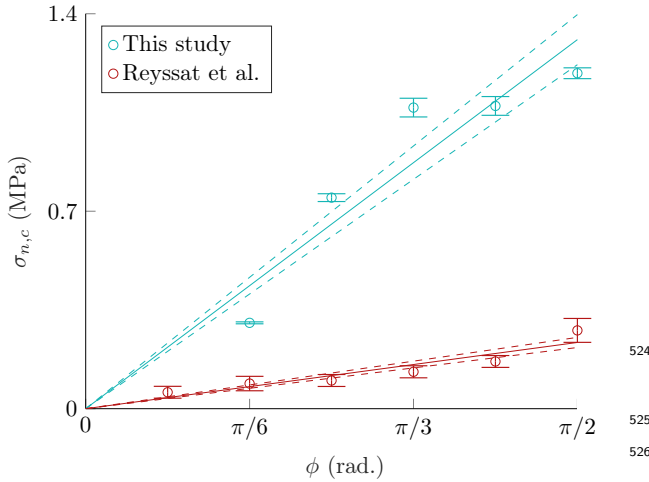


FIG. 8. The normal stress $\sigma_{n,c}$ required for the onset of cutting diminishes with slicing angle ϕ . Our experimental data (blue) as well as data from Reyssat *et al.* are not inconsistent with a linear fit according to Eq. (7): (solid line) derived from the numerical model proposed [11]. The fitted slope is the material parameter $\sigma_{t,c} = 0.84 \pm 0.06$ MPa.

Appendix E: Phase diagram for $h = 28$ mm

Our stress analysis indicates that the free paper height h influences the cutting process (Eq. 56). To quantify how the domains shift, we obtain experimental data

where the paper height is doubled from $h = 14$ mm to $h = 28$ mm. The resulting phase diagram shows that increasing h increases the most hazardous thickness and shifts the corresponding angle ϕ_h downwards (Fig. 9).

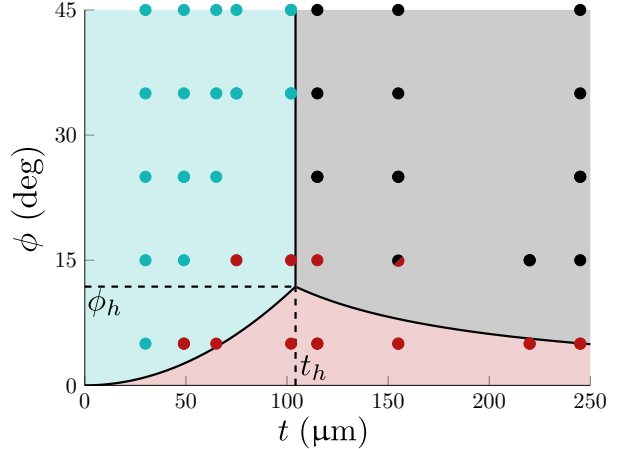


FIG. 9. Phase diagram constructed for paper height $h = 28$ mm, i.e. twice the height used to construct the phase diagram in Figure 3. Peaks at the most hazardous thickness $t_h \approx 105 \mu\text{m}$ (between printed magazines and office paper) and angle $\phi_h \approx 12$ degrees.

Appendix E

TABLE 1: Paper samples used in our experiments. The error is $\pm 5 \mu\text{m}$ for the thickness measurements.

Product	Brand	Area density g/m ²	t μm	E_p MPa
Tissue	Creativ Co.	12.7 ± 1.8	30	0.4 ± 0.3
Printed magazine	Nature	48.8 ± 0.2	49	7.1 ± 1.2
Printed magazine	Science	56.9 ± 1.2	55	7.2 ± 1.6
Newspaper	Information	41.6 ± 0.7	65	8.1 ± 1.8
Dot matrix	Top List	56.6 ± 0.6	65	4.1 ± 1.8
Post its	Stick'n	60.5 ± 0.3	75	9.2 ± 0.2
Office paper	Multicopy	79.6 ± 0.5	102	3.3 ± 1.8
Card stock	Panduro	89 ± 2	115	2.7 ± 0.3
Office paper	ColorChoice	158.3 ± 1.5	155	4.8 ± 1.1
Metallic paper	Panduro	123.9 ± 1.0	165	3 ± 2
Photo paper	Bog & Ide	184 ± 3	220	1.7 ± 0.4
Office paper	Xerox	241.9 ± 1.8	245	3.2 ± 0.8